

Spin-wave dispersion in half-doped $\text{La}_{3/2}\text{Sr}_{1/2}\text{NiO}_4$

D. X. Yao¹ and E. W. Carlson²

(1) Dept. of Physics, Boston University, Boston, MA 02215

(2) Dept. of Physics, Purdue University, West Lafayette, IN 47907

(Dated: September 12, 2006)

Recent neutron scattering measurements reveal spin and charge ordering in the half-doped nickelate, $\text{La}_{3/2}\text{Sr}_{1/2}\text{NiO}_4$. Many of the features of the magnetic excitations have been explained in terms of the spin waves of diagonal stripes with weak single-ion anisotropy. However, an optical mode dispersing away from the (π, π) point was not captured by this theory. We show here that this apparent optical mode is a natural consequence of stripe twinning in a diagonal stripe pattern with a magnetic coupling structure which is two-fold symmetric, *i.e.* one possessing the same spatial rotational symmetry as the ground state.

PACS numbers: 75.30.Ds, 75.10.Hk, 71.27.+a

Strongly correlated electronic systems often exhibit some evidence of charge, spin, or orbital order, or some combination thereof. The interplay between these degrees of freedom can lead to a wide variety of novel phases. The nickelates in particular show a wide range of doping in which both charge and spin order coexist in stripe patterns. The less-ordered stripe structures in some families of cuprates have been widely studied for their possible connection to high temperature superconductivity.

Recent experiments on doped $\text{La}_{2-x}\text{Sr}_x\text{NiO}_4$ have shown clear evidence of static diagonal charge and spin stripe order.[1, 2] Spin wave theory has been successful at describing much of the behavior in these spin-ordered systems.[3, 4, 5, 6, 7, 8] We consider here the recent experiments by Freeman *et al.* on the spin dynamics of half-doped $\text{La}_{3/2}\text{Sr}_{1/2}\text{NiO}_4$ using inelastic neutron scattering.[8] In this material, the spins are in a diagonal stripe phase, where stripes run 45° from the Ni-O bond direction, and the charged domain walls are only 2 lattice constants apart. The charge density modulation can either be considered as densely packed stripes, or as a checkerboard, for domain walls centered on the Ni sites, since in that case the two ways of describing the charge pattern are indistinguishable at this filling. However, if the domain walls are centered on oxygen sites (*i.e.* for bond-centered stripes), the charge checkerboard description is not applicable.

In this paper, we are interested in the extra magnetic mode dispersing away from the antiferromagnetic wavevector $Q_{\text{AF}} = (0.5, 0.5)$ above 50meV in Fig. 3 of Ref. 8. One explanation put forth by the authors is that diagonal discommensurations in the spin order may be able to account for this extra scattering mode. We show here that the mode could also be due to asymmetry in the spin coupling constants, in which case the “extra mode” is really an extension of the acoustic band, made visible due to stripe twinning.

The observed ordering vector is $Q = (0.275, 0.275)$, which is close to a commensurate stripe value of $Q =$

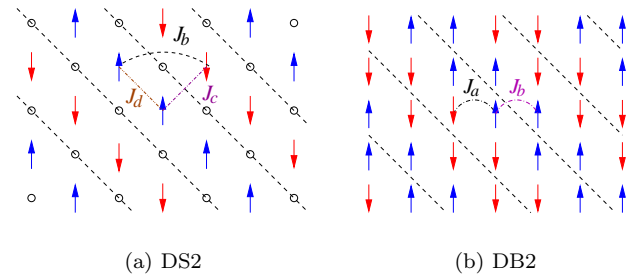


FIG. 1: (Color online) Spin-charge ordering in a NiO_2 square lattice. Arrows represent spins on Ni^{2+} sites and circles represent Ni^{3+} holes. (a) DS2: Diagonal, site-centered stripes of spacing $p = 2$. Note that in this configuration the charges distribution is symmetric under 90° rotations, and is equivalent to a checkerboard pattern. The spin configuration is symmetric under 180° rotations, and breaks the symmetry of the charge checkerboard. The straight-line exchange coupling across the charge domain wall is J_b , and J_c and J_d are diagonal couplings perpendicular and parallel to the charge domain wall, respectively. (b) DB2: Diagonal, bond-centered stripes of spacing $p = 2$. Here, both the charge and spin patterns are 2-fold rotationally symmetric.

$(0.25, 0.25)$. The slight deviation from commensurability is believed to be due to the discommensurations described above. Since we are interested in describing relatively high energy effects, in what follows we neglect the small incommensurability, and consider commensurate diagonal stripe structures of spacing $p = 2$. We consider two patterns in this paper: site-centered stripes as shown in Fig. 1(a), and the corresponding bond-centered stripes shown in Fig. 1(b).

To model these two systems, we use a suitably parametrized Heisenberg model on a square lattice,

$$H = \frac{1}{2} \sum_{i,j} J_{i,j} \mathbf{S}_i \cdot \mathbf{S}_j \quad (1)$$

where the indices i and j run over all sites, and the couplings $J_{i,j}$ are illustrated in Fig. 1. For diagonal, site-

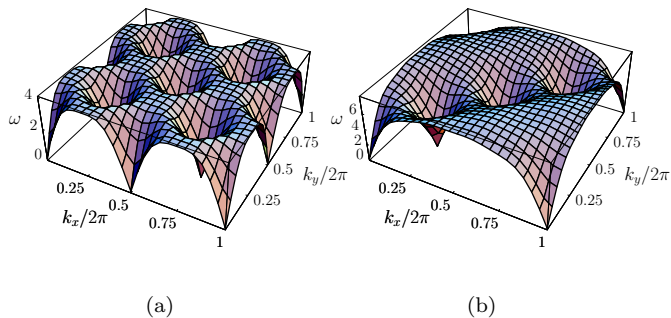


FIG. 2: Band structures of diagonal site-centered stripes (DS2). (a) $J_c = J_d = 0$; (b) $J_c = J_b$, $J_d = -0.5J_b$.

centered stripes of spacing $p = 2$ (DS2), there is no need for nearest-neighbor coupling, and so we set $J_a = 0$. The straight-line coupling J_b across the domain wall is antiferromagnetic. The diagonal coupling J_c across the domain wall is also antiferromagnetic, but the diagonal coupling J_d parallel to the stripes we take to be ferromagnetic, $J_d < 0$, as explained below. In the diagonal bond-centered case (DB2), the nearest neighbor coupling $J_a > 0$ is finite and antiferromagnetic. We also include the ferromagnetic coupling $J_b < 0$ across the domain wall. Since we are interested in describing high energy effects, we neglect the very weak single-ion anisotropy term, which splits the 2-fold degenerate acoustic band at low energy, with one mode remaining gapless at the IC point $Q_{\text{IC}} = (0.25, 0.25)$, and the other mode developing a small gap.[8]

For the case of site-centered stripes in the absence of the diagonal couplings, *i.e.* for $J_c = J_d = 0$, the spin system reduces to two interpenetrating antiferromagnets, with two separate Néel vectors but identical Néel ordering temperatures. Any weak diagonal coupling is sufficient to establish a unique relative direction between the two Néel vectors, and the ground state becomes the stripe structure shown in Fig. 1(a). The number of reciprocal lattice vectors is also decreased by a factor of 2 in the presence of the diagonal couplings $J_c \neq 0$ or $J_d \neq 0$, as can be seen in the bandstructure of Fig. 2. In either case, independent of the value of J_c and J_d , although the antiferromagnetic point Q_{AF} is a magnetic reciprocal lattice vector and therefore must have a spin wave cone dispersing out of it, there is no net antiferromagnetism in the system, so that weight is forbidden at zero frequency at Q_{AF} . The cone that emanates out of Q_{AF} gains finite weight as energy is increased, but remains faint at low energies.

Another key feature of nonzero couplings J_c and J_d for site-centered stripes is the symmetry of the spin wave structure, as shown in Fig. 2. In the limit where $J_c = J_d = 0$, the spin wave dispersion is symmetric under 90° rotations, as shown in Fig. 2(a). However, when

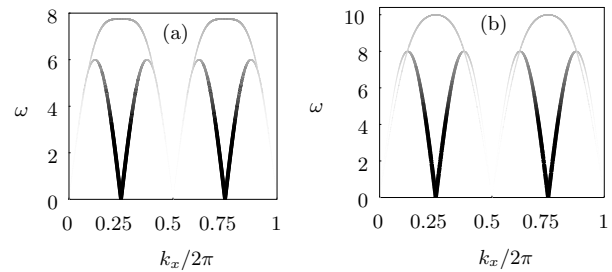


FIG. 3: DS2: Diagonal, site-centered stripes of spacing $p = 2$. The plots are for twinned stripes, summing contributions along (k_x, k_x) and $(k_x, -k_x)$. (a) $J_c = J_b$ and $J_d = -0.5J_b$; (b) $J_c = 2J_b$ and $J_d = -0.5J_b$.

either J_c or J_d or both are nonzero, the symmetry is broken, and the spin wave structure is now only symmetric under 180° rotations, as shown in Fig. 2(b). This means that for any nonzero J_c or J_d , the spin wave velocity of the acoustic mode dispersing out of $Q_{\text{AF}} = (0.5, 0.5)$ is different parallel and perpendicular to the stripe direction. In the presence of stripe twins, the two velocities will appear as two branches in plots of ω vs. \vec{k} , as shown in Fig. 3.

The magnon dispersion from Eq. (1) can be solved analytically, and for DS2 we find that

$$\omega(k_x, k_y) = 2\sqrt{A^2 - B^2}, \quad (2)$$

where

$$\begin{aligned} A &= 2J_b + J_c - J_d + J_d \cos(k_x - k_y) \\ B &= J_b \cos(2k_x) + J_b \cos(2k_y) + J_c \cos(k_x + k_y). \end{aligned} \quad (3)$$

There are two different spin wave velocities for the cones emanating from the IC peak $Q_{\text{IC}} = (0.25, 0.25)$ and symmetry-related points, one corresponding to spin wave velocities perpendicular to the direction of the domain walls (*i.e.* perpendicular to the stripes), and the other parallel to the direction of the domain walls,

$$\begin{aligned} v_{\perp} &= 4(2J_b + J_c) \\ v_{\parallel} &= 4\sqrt{(2J_b + J_c)(2J_b - J_d)}. \end{aligned} \quad (4)$$

In Fig. 3, we show the expected dispersions and scattering intensities for DS2. Plots are shown for twinned stripes, summing the contributions parallel and perpendicular to the stripe direction, *i.e.* along the $(k_x, -k_x)$ and (k_x, k_x) directions, respectively. Because J_c and J_d are nonzero, there is an apparent optical mode. Note that it is not a true optical mode, since in this configuration there are only two spins per unit cell, leading to only one (twofold degenerate) band. As in the bond-centered case, weight is forbidden at low energy at the antiferromagnetic point Q_{AF} , so that the spin-wave cone emanating from this magnetic reciprocal lattice vector

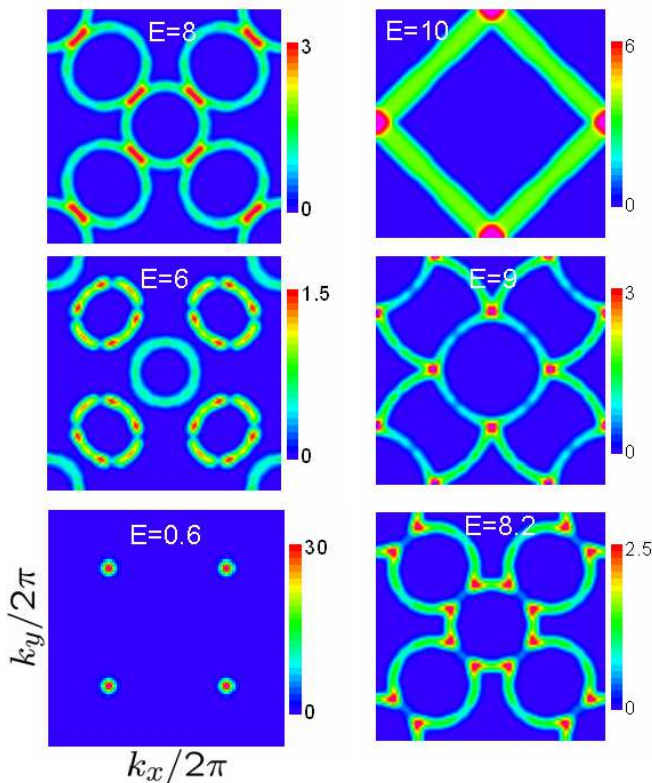


FIG. 4: (Color online) Constant energy cuts with windows of $0.1J_b S$ for twinned diagonal, site-centered stripes of spacing $p = 2$ at $J_c = 2J_b$ and $J_d = -0.5J_b$. The energy E is in units of $J_b S$.

has vanishing weight as $\omega \rightarrow 0$. In Fig. 3(a), we have set $J_c = J_b$ and $J_d = -0.5J_b$. In Fig. 3(b), we use $J_c = 2J_b$ with $J_d = -0.5J_b$. Notice that in panel (a) of the figure, the apparent optical mode is flat.

We have chosen the coupling constants with the following in mind: The “acoustic” branch peaks at $\omega(3\pi/4, 3\pi/4) = 4J_b + 2J_c$. The apparent “optical” mode peaks at $\omega(\pi/2, 3\pi/2) = 4\sqrt{(2J_b - J_d)(J_c - J_d)}$. The data indicate that the apparent optical mode is higher in energy than the top of the “acoustic” part: $\omega(\pi/2, 3\pi/2) > \omega(3\pi/4, 3\pi/4)$, which implies that

$$J_d \leq (1/2)(2 + J_c - \sqrt{2}\sqrt{4 + J_c^2}) \quad (5)$$

when $J_b = 1$. However, the extra mode above 50meV is not too high in energy, so parameters need to be chosen so as to satisfy this constraint, but remain close to the equality.

We also require the apparent “optical” branch to be concave, since there is no evidence of a dip in the extra mode. This requirement gives

$$\frac{\partial^2}{\partial k_x^2} \omega(k_x, -k_x) = \frac{4(J_d - 2)(J_c - 2 - 2J_d)}{\sqrt{-(J_c - J_d)(J_d - 2)}} \leq 0, \quad (6)$$

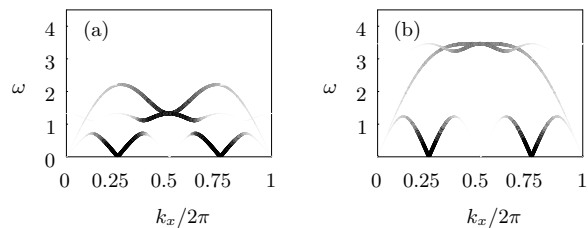


FIG. 5: DB2: Diagonal, bond-centered stripes of spacing $p = 2$. (See Fig. 1(b).) The plots are for twinned stripes, summing contributions along (k_x, k_x) and $(k_x, -k_x)$. (a) Very weak coupling across the domain wall, with $J_b = -0.1J_a$. (b) Weak coupling across the domain wall, with $J_b = -0.5J_a$.

resulting in the constraint that

$$J_d \leq \frac{1}{2}J_c - 1. \quad (7)$$

As long as the second constraint, Eqn. 7, is satisfied in the range $0 \leq J_c \leq 2J_b$, then the first constraint, Eqn. 5, is also satisfied. To describe the data, then, we find that we need a sizeable J_c , on the order of J_b . This makes J_c significantly larger than that reported at the lower doping $x = 1/3$, where diagonal site-centered stripes of spacing $p = 3$ (DS3) were used to explain the data successfully.[2] Although the fits in Ref. 2 were good for $J_c = 0$ and were not significantly improved by letting J_c increase to $J_c \approx 0.5J_b$, the data were still well described using a nonzero J_c . We find that the data at doping $x = 1/3$ are also well described by taking J_c to be as large as J_b or even $2J_b$ as in our Fig. 3.

We also find that we need $J_d < 0$, *i.e.* the diagonal coupling parallel to the stripes needs to be ferromagnetic, in order to describe the data. If one considers the diagonal spin couplings J_c and J_d to be derived from, *e.g.*, a perturbative treatment of a single-band Hubbard or three-band Emery model on a square Ni-O lattice, we expect $J_c = J_d$. Given that the spin ground state breaks the 4-fold rotational symmetry of the square lattice to only 2-fold rotational symmetry, any finite spin-lattice coupling results in the two diagonal directions being inequivalent, and leads to $J_c \neq J_d$. For weak rotational symmetry breaking of the square lattice in the perturbative regime, one expects $J_c = J_o + \epsilon$ with $J_d = J_o - \epsilon$ where ϵ is small compared to J_o , so that the anisotropy between the two diagonal coupling directions is weak as well. (This preserves the spin ground state of Fig. 1(a).) We find, however, that this regime of the coupling constants leads to the apparent optical mode being too low in energy to capture the data. This may indicate that the materials are far from the perturbative limit of the single-band Hubbard or three-band Emery model.

Fig. 4 shows constant energy cuts for DS2 corresponding to the parameters in Fig. 3(b). An important feature of this configuration is that although the antiferromagnetic point $Q_{AF} = (0.5, 0.5)$ is a magnetic reciprocal

lattice vector, zero-frequency weight is forbidden there by symmetry, since the stripes have no net Néel vector at Q_{AF} . Combined with the fact that there is no optical band, the DS2 configuration *can never have spectral weight at the antiferromagnetic point* Q_{AF} , even at finite frequency. Notice that as energy is increased in Fig. 4, a faint spin wave cone emerges from Q_{AF} in a light ring of scattering, but none of the constant energy plots show any weight at Q_{AF} . This is consistent with the constant energy plots for $\text{La}_{3/2}\text{Sr}_{1/2}\text{NiO}_4$ shown in Ref. 8. By contrast, the corresponding bond-centered configuration (DB2) shown in Fig. 1(b) has an optical band which displays a saddlepoint at Q_{AF} , and rather large scattering intensity at finite frequency at Q_{AF} as a result. (See Fig. 5 of this paper, as well as Fig. 8 of our previous paper, Ref. 4.)

While diagonal, site-centered stripes of spacing $p = 2$ (DS2) are able to account for the behavior of the apparent optical mode observed to disperse away from Q_{AF} in Fig. 3 of Freeman *et al.*[8], there are two other high energy features which this model has not captured. One is the asymmetry in intensity observed above 30meV in the spin wave cones emanating from the main IC peaks. The other is a mode in the 31 – 39meV range propagating away from (h, k) structural reciprocal lattice points. These (as well as the apparent optical mode) have been attributed to discommensurations in the magnetic order.[8]

In Fig. 5, we show the expected dispersions and intensities for the diagonal, *bond-centered* stripes (DB2) shown in Fig. 1(b). This configuration has a true optical mode. Fig. 5(a) shows weak coupling across the charged domain walls, with $J_b = -0.1J_a$, and Fig. 5(b) has somewhat stronger coupling across the domain walls, with $J_b = -0.5J_a$. Note that in the bond-centered case, couplings across the domain walls are ferromagnetic. Results are shown for twinned stripe patterns, summing the contribution parallel and perpendicular to the stripe direction, *i.e.* along the $(k_x, -k_x)$ and (k_x, k_x) directions, respectively. Although there is a reciprocal lattice vector at Q_{AF} , weight is forbidden there at zero frequency, since the Néel vector switches sign across the domain walls. We have reported the analytic form of the spin wave dispersion in this case in a previous publication.[3]

Because this spin configuration is only 180° symmetric, the spin-wave velocity emanating from Q_{AF} is different parallel and perpendicular to the stripe direction. However, the branch emanating from Q_{AF} in the direction parallel to stripes has so little weight as to be effectively invisible in the plots. This configuration displays a true optical mode because there are four spins in the unit cell. The optical mode has a *saddlepoint* at Q_{AF} and finite energy, with increased weight at the saddlepoint. For weak coupling across the domain walls ($|J_b| < |J_a|$), the optical mode always displays significant weight at Q_{AF} at finite frequency. This is not supported by the data[8],

which at the energies measured display no scattering at Q_{AF} and finite frequency. This likely indicates that the domain walls are not bond-centered in this material, but are probably site-centered.

In conclusion, we have used linear spin-wave theory to describe the magnetic excitations recently observed in neutron scattering[8] on $\text{La}_{3/2}\text{Sr}_{1/2}\text{NiO}_4$. Many features of the data were captured in the spin wave analysis of Ref. 8. Other features, including an apparent optical mode dispersing away from Q_{AF} above 50meV, were attributed to discommensurations in the spin order. We show here that the apparent optical mode may also be captured in linear spin wave theory by using a spin coupling configuration that preserves the symmetry of the spin ground state. Namely, we have shown that diagonal, site-centered stripes of spacing $p = 2$ capture this mode when the pattern of couplings is 2-fold symmetric. This is because the 2-fold symmetric coupling pattern gives rise to two different spin-wave velocities (*i.e.* $v_{\parallel} \neq v_{\perp}$) emanating from the antiferromagnetic point $Q_{AF} = (0.5, 0.5)$. For twinned samples, the two velocities are simultaneously visible, and the higher velocity mode v_{\parallel} parallel to the stripes is responsible for the “extra” scattering above 50meV. Furthermore, this configuration is forbidden to display scattering at the antiferromagnetic point Q_{AF} , whereas bond-centered stripes have a true optical mode with significant weight at Q_{AF} , which is not supported by the data. We therefore conclude that the magnetic excitations observed in Ref. 8 are consistent with site-centered stripes, but not with bond-centered stripes..

It is a pleasure to thank D. K. Campbell and A. T. Boothroyd for helpful discussions. This work was supported by Boston University (DXY), and by the Purdue Research Foundation (EWC). EWC is a Cottrell Scholar of Research Corporation.

-
- [1] A. T. Boothroyd, D. Prabhakaran, P. G. Freeman, S. J. S. Lister, M. Enderle, A. Hiess, and J. Kulda, Phys. Rev. B **67**, 100407(R) (2003).
 - [2] H. Woo, A. T. Boothroyd, K. Nakajima, T. G. Perring, C. Frost, P. G. Freeman, D. Prabhakaran, K. Yamada, and J. M. Tranquada, Phys. Rev. B **72**, 064437 (2005).
 - [3] E. W. Carlson, D. X. Yao, and D. K. Campbell, Phys. Rev. B **70**, 064505 (2004).
 - [4] D. X. Yao, E. W. Carlson, and D. K. Campbell, Phys. Rev. B **73**, 224525 (2006).
 - [5] J. M. Tranquada, P. M. Gehring, G. Shirane, S. Shamoto, and M. Sato, Phys. Rev. B **46**, 5561 (1992).
 - [6] P. Bourges, Y. Sidis, M. Braden, K. Nakajima, and J. M. Tranquada, Phys. Rev. Lett. **90**, 147202 (2003).
 - [7] F. Krüger and S. Scheidl, Phys. Rev. B **67**, 134512 (2003).
 - [8] P. G. Freeman, A. T. Boothroyd, D. Prabhakaran, C. Frost, M. Enderle, and A. Hiess, Phys. Rev. B **71**, 174412 (2005).